Arch. Metall. Mater. **70** (2025), 2, 1233-1236

DOI: https://doi.org/10.24425/amm.2025.154472

P. REZAEI-SHAHREZA[1*], S. HASANI[1], A. SEIFODDINI[1], M. NABIAŁEK[2]

STRUCTURAL STABILITY AND GLASS-FORMING ABILITY OF $Fe_{74}B_{20}Nb_2Hf_2Si_2$: THE ROLE OF COOLING RATE

This study investigates the effect of cooling rate on the glass transition behavior of the $Fe_{74}B_{20}Nb_2Hf_2Si_2$ soft magnetic amorphous alloy. Rectangular samples with two different dimensions, 70.0 mm × 1.0 mm × 1.0 mm, and 50.0 mm × 30.0 mm × 0.5 mm, were prepared and analyzed using X-ray diffraction (XRD) and differential scanning calorimetry (DSC). XRD results confirmed the amorphous nature of the alloy, evidenced by a broad peak in the 2θ range of 35-50°. The glass-forming ability (GFA) parameters, including $\Delta T_x = T_x - T_g$ and $T_{rx} = T_x/T_g$, were derived from DSC curves, where T_g represents the glass transition temperature and T_x denotes the crystallization onset temperature. A notable increase in ΔT_x from 43 to 52 K was observed with a decreasing cooling rate, signifying enhanced structural stability in the sample with dimensions of 70.0 mm × 1.0 mm × 1.0 mm compared to the sample with dimensions of 50.0 mm × 30.0 mm × 0.5 mm. Additionally, the sample with dimensions of 70.0 mm × 1.0 mm × 1.0 mm exhibited lower free volume (FV = 141.2 J/g) and heat capacity (ΔC_p = 0.037 J/g. K) compared to the sample with dimension of 50.0 mm × 30.0 mm × 0.5 mm (FV = 174.7 J/g and ΔC_p = 0.145 J/g. K). These findings suggested that slower cooling rates contribute to the structural stability of the amorphous alloy by minimizing defects and lowering heat capacity, potentially improving its performance in magnetic applications.

Keywords: Amorphous alloy; Glass-forming ability; Thermal analysis; Free volume; Heat capacity

1. Introduction

The improvement of glass-forming ability (GFA) in amorphous alloys, particularly Fe-based alloys, has become a pivotal focus within the field of materials science. This is largely due to the significant influence GFA on the structural, thermal, and mechanical properties of these materials [1-4]. Alloys with high GFA exhibit a strong tendency to form amorphous phases, effectively preventing the formation of unwanted crystals during manufacturing processes [5-8]. This leads to improved thermal stability and resistance to temperature fluctuations. Furthermore, alloys with optimized GFA offer easier and more cost-effective production, reducing the need for complex process controls and minimizing manufacturing costs [9-12]. Various strategies have been proposed to enhance GFA, including modifications to chemical composition, increasing component thickness, environmental control, and optimization of processing parameters [13-16]. One effective approach is increasing the thickness of the component, which, due to the larger volume of material, reduces the cooling rate and allows more time for the formation of the amorphous phase [17-19].

In this context, a soft magnetic amorphous alloy with the composition $Fe_{74}B_{20}Nb_2Hf_2Si_2$ was produced in the form of rectangular samples with different dimensions of 70.0 × 1.0 × 1.0 mm and 50.0 × 0.5 × 0.5 mm. Then, the effect of cooling rate on the alloy's GFA was evaluated using X-ray diffraction (XRD) and differential scanning calorimetry (DSC) analyses.

2. Experimental

The alloy with a composition of $Fe_{74}B_{20}Nb_2Hf_2Si_2$ (at.%) was prepared using high-purity elements (99.9999%) through vacuum arc melting in a titanium-gettered argon atmosphere. To ensure compositional homogeneity, the melting process was repeated five times. Rectangular samples with different dimensions were fabricated by water-cooled copper mold casting using the injection casting technique. The dimentions of samples were 70.0 mm × 1.0 mm × 1.0 mm for Sample A, and 50.0 mm × 30.0 mm × 0.5 mm for Sample B.

The amorphous structure of both samples was confirmed through XRD analysis using a Bruker D8 diffractometer with

[1] YAZD UNIVERSITY, DEPARTMENT OF MINING AND METALLURGICAL ENGINEERING, 89195-741, YAZD, IRAN
[2] CZĘSTOCHOWA UNIVERSITY OF TECHNOLOGY, DEPARTMENT OF PHYSICS, ARMII KRAJOWEJ 19 AV., 42-200 CZĘSTOCHOWA, POLAND
* Corresponding author: parisarezaei88@yahoo.com

copper (Cu k_α, λ = 0.15418 nm) radiation. Furthermore, the thermal behavior of the samples was evaluated using low-temperature DSC, performed on a Netzsch DSC 214 Polyma at a heating rate of 20 K/min.

3. Results and dscussions

The XRD pattern of both samples A and B in their as-cast state are presented in Fig. 1. As illustrated, a broad peak is observed in the 2θ range of 35 to 50°, which is characteristic of the amorphous nature of the samples. Although Sample B exhibits minor low-intensity reflections around 45° and 58°, these do not correspond to distinct crystalline phases and could be attributed to short-range ordering or minor structural fluctuations. Overall, the XRD results confirm that the predominant structure of both samples remains amorphous.

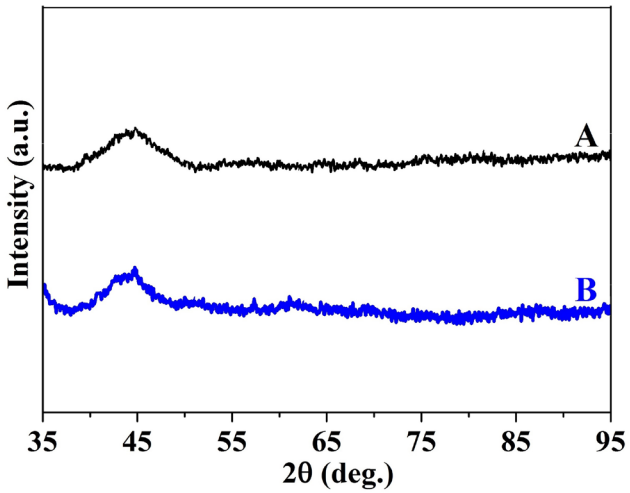

Fig. 1. XRD patterns for both samples in the as-cast state

Fig. 2 presents the DSC curves of the alloy in its as-cast state for both Samples A and B. The critical temperatures, including the glass transition temperature (T_g) and the onset of crystallization temperature (T_x), were extracted from the DSC curves and are summarized in TABLE 1. Notably, the T_g of Sample A (659 K) is higher than Sample B (644 K).

This difference can be attributed to the reduced cooling rate in Sample A, which allows more time for atomic arrangements, resulting in a structure that is closer to a more ordered state. Consequently, this increases the energy required for the transition into the supercooled liquid phase. Additionally, the reduced cooling rate enhances density and structural order, thereby stabilizing the amorphous phase. As a result, a higher T_g is observed, as more energy is needed to disrupt the ordered structure and transition to the liquid state [20,21].

TABLE 1

Summary of key parameters related to the GFA of both samples A and B

Sample	T_g (K)	T_x (K)	ΔT_x (K)	T_{rx}	FV (J/g)
A	659	711	52	1.13	141.2
B	644	687	43	1.11	174.7

The GFA parameters, including $\Delta T_x = (T_x - T_g)$ and $T_{rx} = (T_x/T_g)$, are also listed in Table 1 for samples A and B. The data indicate that Sample A exhibits higher values of ΔT_x (52 K) and T_{rx} (1.13), suggesting an enhanced GFA compared to Sample B. This improvement can be attributed to the lower cooling rate in Sample A, which facilitates better atomic organization and results in increased thermal stability and higher T_x values. Additionally, the slower cooling rate minimizes structural defects and enhances order within the amorphous structure, thus requiring more energy to initiate crystallization [22,23]. Consequently, the increased gap between T_g and T_x, reflected in the higher ΔT_x and T_{rx} values, signifies improved stability of the amorphous phase and its greater resistance to crystallization.

Another critical factor in evaluating GFA is the free volume (FV), which can be assessed through enthalpy changes near

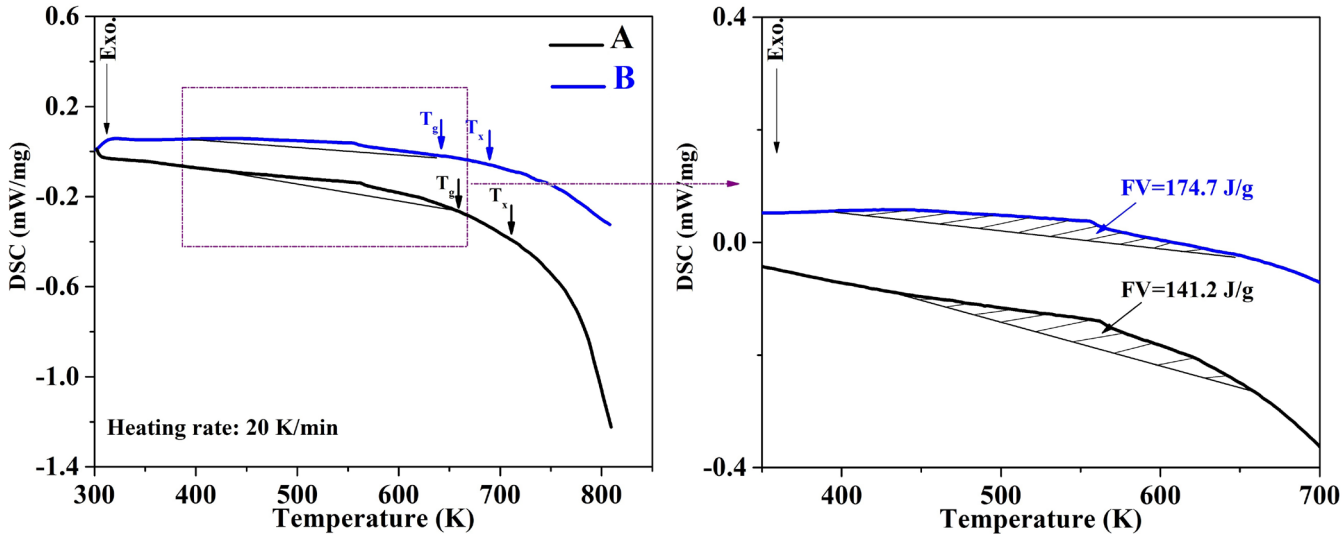

Fig. 2. Low temperature DSC curves related to the investigated samples at a heating rate of 20 K/min

the T_g using DSC analysis, as depicted in Fig. 1. According to TABLE 1, the *FV* value for Sample A decreases from 174.7 to 141.2 J/g compared to Sample B. This reduction in free volume results from the slower cooling rate in sample A, which allows more time for atomic organization and, consequently, reduces structural defects and atomic mobility [24-26].

As a result, the liquid phase becomes more stable, diminishing the driving force for crystallization. Additionally, the decrease in free volume lowers both the entropy of fusion and the Gibbs free energy difference (ΔG_c) between the supercooled liquid and crystalline phases, making crystallization less probable and enhancing the stability of the amorphous phase [27,28]. Therefore, the GFA of Sample A is superior to that of Sample B.

In addition to the factors previously discussed, the heat capacity (ΔC_p) at T_g is a key parameter for assessing the stability of the amorphous structure. The ΔC_p values for Samples A and B, calculated using Proteus software, are 0.037 and 0.145 J/g·K, respectively. The lower ΔC_p observed in Sample A correlates with its reduced cooling rate and increased GFA.

A decreased heat capacity suggests lower atomic mobility near T_g, which enhances the stability of the amorphous phase and inhibits crystallization [29-31]. Moreover, lower ΔC_p values indicate reduced entropy and increased viscosity, further contributing to improved GFA. Also, the decrease inactivation energy required to maintain the amorphous structure lowers the likelihood of crystallization under thermal stress [32,33].

At lower cooling rates, the alloy's structure gains more time to organize and reduce structural defects, thereby improving the overall stability of the glass. Therefore, the combined effects of reduced heat capacity and slower cooling rates significantly enhance the GFA of the amorphous alloy.

4. Conclusion

This study demonstrates that the $Fe_{74}B_{20}Nb_2Hf_2Si_2$ amorphous alloy exhibits superior GFA in rectangular samples with different dimensions of 70.0 mm × 1.0 mm × 1.0 mm, and 50.0 mm × 30.0 mm × 0.5 mm. XRD analysis confirmed the amorphous structure in both samples, while DSC results revealed a higher T_g in the sample with dimensions of 70.0 mm × 1.0 mm × 1.0 mm, indicating increased structural stability due to the slower cooling rate. The higher values of ΔT_x and T_{rx} in the same sample further confirm its enhanced thermal stability and resistance to crystallization. Additionally, a reduction in free volume, as determined through enthalpy analysis, contributes to the improved GFA by minimizing structural defects and reducing the driving force for crystallization. The lower ΔC_p observed in the sample with dimensions of 70.0 mm × 1.0 mm × 1.0 mm suggests decreased atomic mobility and higher viscosity, resulting in a more stable amorphous structure.

These findings highlight that by controlling the cooling rate and optimizing the alloy's structural characteristics, the GFA of amorphous alloys can be significantly enhanced, leading to improved thermal stability and resistance to crystallization.

REFERENCES

[1] P. Rezaei-Shahreza, S. Hasani, A. Seifoddini, M. Nabiałek, P. Czaja, A. Śliwa, Viscosity of the supercooled liquid and crystallization kinetic analysis in the Fe74B20Nb2Hf2Si2 amorphous alloy. Intermetallics **161**, 107971 (2023). DOI: https://doi.org/10.1016/j.intermet.2023.107971

[2] B. Jeż, Influence of the Cooling Rate on the Heterogeneity of the Structure in the Rapid Quenched Fe – Based Alloys with the Si Addition. Arch. Metall. Mater. **69**, 1, 231-235 (2024). DOI: https://doi.org/10.24425/amm.2024.147813

[3] M. Nabiałek, B. Jeż, K. Błoch, P. Pietrusiewicz, J. Gondro, The effect of the cobalt-content on the magnetic properties of iron-based amorphous alloys. J. Magn. Magn. Mater. **477**, 214-219 (2019). DOI: https://doi.org/10.1016/j.jmmm.2019.01.073

[4] P. Rezaei-Shahreza, S. Hasani, A. Seifoddini, M. Nabiałek, P. Czaja, The crystallization process in a new multicomponent Fe-based bulk amorphous alloy: A kinetic study approach. Mater. Charact. **196**, 112602 (2023). DOI: https://doi.org/10.1016/j.matchar.2022.112602

[5] P. Rezaei-Shahreza, A. Seifoddini, S. Hasani, Thermal stability and crystallization process in a Fe-based bulk amorphous alloy: The kinetic analysis. J. Non. Cryst. Solids **471**, 286-294 (2017). DOI: https://doi.org/10.1016/j.jnoncrysol.2017.05.044

[6] M. Nabiałek, B. Jeż, K. Błoch, The Influence of the Silicon Content on the Formation of Fe23B6 Metastable Phases in Fe65Co11−xB-20SixZr2Hf2 Bulk Amorphous Alloys. Metall. Mater. Trans. A. **51**, 4602-4609 (2020). DOI: https://doi.org/10.1007/s11661-020-05894-y

[7] S. Hasani, P. Rezaei-Shahreza, A. Seifoddini, M. Hakimi, Enhanced glass forming ability, mechanical, and magnetic properties of Fe 41 Co 7 Cr 15 Mo 14 Y 2 C 15 B 6 bulk metallic glass with minor addition of Cu. J. Non. Cryst. Solids **497**, 40-47 (2018). DOI: https://doi.org/10.1016/j.jnoncrysol.2018.05.021

[8] J. Olszewski, J. Zbroszczyk, K. Sobczyk, W. Ciurzyńska, P. Brągiel, M. Nabiałek, J. Świerczek, M. Hasiak, A. Łukiewska, Thermal Stability and Crystallization of Iron and Cobalt - Based Bulk Amorphous Alloys. Acta Phys. Pol. A. **114**, 659-1666 (2008). DOI: https://doi.org/10.12693/APhysPolA.114.1659

[9] D.K. Rajak, P.H. Wagh, E. Linul, Manufacturing Technologies of Carbon/Glass Fiber-Reinforced Polymer Composites and Their Properties: A Review. Polymers (Basel). **13**, 3721 (2021). DOI: https://doi.org/10.3390/polym13213721

[10] M. Nabiałek, B. Jeż, K. Błoch, J. Gondro, K. Jeż, A.V. Sandu, P. Pietrusiewicz, Relationship between the shape of X-ray diffraction patterns and magnetic properties of bulk amorphous alloys Fe65Nb5Y5+xHf5-xB20 (where: x = 0, 1,2, 3, 4, 5). J. Alloys Compd. **820**, 153420 (2020). DOI: https://doi.org/10.1016/j.jallcom.2019.153420

[11] W.H. Ryu, K.J. Kim, M.K. Kwak, C.W. Ryu, E.S. Park, Development of Zr-based metallic glasses to utilize thermoplastic forming processes of engineering plastics. Mater. Des. **232**, 112100 (2023). DOI: https://doi.org/10.1016/j.matdes.2023.112100

[12] S. Hasani, P. Rezaei-Shahreza, A. Seifoddini, The effect of Cu minor addition on the non-isothermal kinetic of nano-crystallites

formation in Fe41Co7Cr15Mo14Y2C15B6 BMG. J. Therm. Anal. Calorim. **143**, 3365-3375 (2021).
DOI: https://doi.org/10.1007/s10973-020-09716-6

[13] J. Gondro, J. Świerczek, J. Olszewski, J. Zbroszczyk, K. Sobczyk, W.H. Ciurzyńska, J. Rzącki, M. Nabiałek, Magnetization behavior and magnetocaloric effect in bulk amorphous Fe60Co5Zr8Mo5W2B20 alloy. J. Magn. Magn. Mater. **324**, 1360-1364 (2012).
DOI: https://doi.org/10.1016/j.jmmm.2011.11.038

[14] B. Jeż, J. Wysłocki, S. Walters, P. Postawa, M. Nabiałek, The Process of Magnetizing FeNbYHfB Bulk Amorphous Alloys in Strong Magnetic Fields. Materials (Basel). **13**, 1367 (2020).
DOI: https://doi.org/10.3390/ma13061367

[15] H. Luo, Y. Du, Mechanical Properties of Bulk Metallic Glasses Additively Manufactured by Laser Powder Bed Fusion: A Review. Materials (Basel). **16**, 7034 (2023).
DOI: https://doi.org/10.3390/ma16217034

[16] N. Lebrun, F. Dupla, H. Bruhier, M. Prudent, A. Borroto, C. Der Loughian, F. Bourquard, J.-M. Pelletier, M. Rousseau, J.-P. Colombier, J.-F. Pierson, F. Garrelie, P. Steyer, Metallic glasses for biological applications and opportunities opened by laser surface texturing: A review. Appl. Surf. Sci. **670**, 160617 (2024).
DOI: https://doi.org/10.1016/j.apsusc.2024.160617

[17] Z.P. Lu, C.T. Liu, A new glass-forming ability criterion for bulk metallic glasses. Acta Mater. **50**, 3501-3512 (2002).
DOI: https://doi.org/10.1016/S1359-6454(02)00166-0

[18] Z. Li, Z. Huang, F. Sun, X. Li, J. Ma, Forming of metallic glasses: mechanisms and processes. Mater. Today Adv. **7**, 100077 (2020).
DOI: https://doi.org/10.1016/j.mtadv.2020.100077

[19] N. Li, L. Liu, Q. Chen, J. Pan, K.C. Chan, The effect of free volume on the deformation behaviour of a Zr-based metallic glass under nanoindentation. J. Phys. D. Appl. Phys. **40**, 6055-6059 (2007).
DOI: https://doi.org/10.1088/0022-3727/40/19/043

[20] Y. Roos, M. Karel, Plasticizing Effect of Water on Thermal Behavior and Crystallization of Amorphous Food Models. J. Food Sci. **56**, 38-43 (1991).
DOI: https://doi.org/10.1111/j.1365-2621.1991.tb07970.x

[21] C.M. Grigorian, T.J. Rupert, Critical cooling rates for amorphous-to-ordered complexion transitions in Cu-rich nanocrystalline alloys. Acta Mater. **206**, 116650 (2021).
DOI: https://doi.org/10.1016/j.actamat.2021.116650

[22] X. Guo, Y. Gao, Z. Meng, T. Gao, Effect of Cooling Rate on the Crystal Quality and Crystallization Rate of SiC during Rapid Solidification Based on the Solid–Liquid Model. Crystals **12**, 1019 (2022).
DOI: https://doi.org/10.3390/cryst12081019

[23] M. Mohri, F. Forghani, M. Nili-Ahmadabadi, Structural evolution and thermal stability of functionally graded NiTi nano-glass thin films alloys during crystallization. Mater. Charact. **187**, 111850 (2022). DOI: https://doi.org/10.1016/j.matchar.2022.111850

[24] K. Tao, J.C. Qiao, L. Zhang, J.M. Pelletier, Dynamic mechanical response of ZrCu-based bulk metallic glasses. Int. J. Mech. Sci. **211**, 106770 (2021).
DOI: https://doi.org/10.1016/j.ijmecsci.2021.106770

[25] Z. Evenson, T. Koschine, S. Wei, O. Gross, J. Bednarcik, I. Gallino, J.J. Kruzic, K. Rätzke, F. Faupel, R. Busch, The effect of low-temperature structural relaxation on free volume and chemical short-range ordering in a Au49Cu26.9Si16.3Ag5.5Pd2.3 bulk metallic glass. Scr. Mater. **103**, 14-17 (2015).
DOI: https://doi.org/10.1016/j.scriptamat.2015.02.026

[26] A.R. Yavari, A. Le Moulec, A. Inoue, N. Nishiyama, N. Lupu, E. Matsubara, W.J. Botta, G. Vaughan, M. Di Michiel, Å. Kvick, Excess free volume in metallic glasses measured by X-ray diffraction. Acta Mater. **53**, 1611-1619 (2005).
DOI: https://doi.org/10.1016/j.actamat.2004.12.011

[27] M. Descamps, E. Dudognon, Crystallization from the Amorphous State: Nucleation–Growth Decoupling, Polymorphism Interplay, and the Role of Interfaces. J. Pharm. Sci. **103**, 2615-2628 (2014).
DOI: https://doi.org/10.1002/jps.24016

[28] L. Yu, S.M. Reutzel-Edens, C.A. Mitchell, Crystallization and Polymorphism of Conformationally Flexible Molecules: Problems, Patterns, and Strategies. Org. Process Res. Dev. **4**, 396-402 (2000). DOI: https://doi.org/10.1021/op000028v

[29] D. Zhou, G.G.Z. Zhang, D. Law, D.J.W. Grant, E.A. Schmitt, Thermodynamics, Molecular Mobility and Crystallization Kinetics of Amorphous Griseofulvin. Mol. Pharm. **5**, 927-936 (2008).
DOI: https://doi.org/10.1021/mp800169g

[30] R. Svoboda, K. Kozlová, Thermo-Structural Characterization of Phase Transitions in Amorphous Griseofulvin: From Sub-Tg Relaxation and Crystal Growth to High-Temperature Decomposition. Molecules **29**, 1516 (2024).
DOI: https://doi.org/10.3390/molecules29071516

[31] J. Zhang, M. Guo, M. Luo, T. Cai, Advances in the development of amorphous solid dispersions: The role of polymeric carriers. Asian J. Pharm. Sci. **18**, 100834 (2023).
DOI: https://doi.org/10.1016/j.ajps.2023.100834

[32] T. Miyazaki, R. Mizoguchi, K. Ueda, T. Shinozaki, M. Kamoto, Y. Takeda, S. Sakuma, N. Ito, M. Momo, K. Kawakami, Crystallization of Amorphous Nifedipine Under Isothermal Conditions: Inter-laboratory Reproducibility and Investigation of the Factors Affecting Reproducibility. J. Pharm. Sci. **112**, 2703-2716 (2023).
DOI: https://doi.org/10.1016/j.xphs.2023.06.002

[33] K.A. Graeser, J.E. Patterson, J.A. Zeitler, T. Rades, The Role of Configurational Entropy in Amorphous Systems. Pharmaceutics **2**, 224-244 (2010).
DOI: https://doi.org/10.3390/pharmaceutics2020224